FERMILAB-PUB-15-297-TD
(accepted)

Methodology for the Structural Design of Single Spoke Accelerating Cavities at Fermilab

Donato Passarelli[a,b,*], Robert H. Wands[a], Margherita Merio[a], Leonardo Ristori[a]

[a] *Fermi National Accelerator Laboratory, 60510 Batavia, IL, USA*
[b] *Department of Civil and Mechanical Engineering, University of Pisa, 56122 Pisa, Italy*

Abstract

Fermilab is planning to upgrade its accelerator complex to deliver a more powerful and intense proton-beam for neutrino experiments. In the framework of the so-called Proton Improvement Plan-II (PIP-II), we are designing and developing a cryomodule containing superconducting accelerating cavities, the Single Spoke Resonators of type 1 (SSR1). In this paper, we present the sequence of analysis and calculations performed for the structural design of these cavities, using the rules of the American Society of Mechanical Engineers (ASME) Boiler and Pressure Vessel Code (BPVC). The lack of an accepted procedure for addressing the design, fabrication, and inspection of such unique pressure vessels makes the task demanding and challenging every time. Several factors such as exotic materials, unqualified brazing procedures, limited nondestructive examination, and the general R&D nature of these early generations of cavity design, conspire to make it impractical to obtain full compliance with all ASME BPVC requirements. However, the presented approach allowed us to validate the design of these new generation of single spoke cavities with values of maximum allowable working pressure that exceed the safety requirements. This set of rules could be used as a starting point for the structural design and development of similar objects.

Keywords:
LINAC, SRF, Single Spoke Resonators, Pressure vessels, ASME Code

*Corresponding author.
Email address: donato@fnal.gov (Donato Passarelli)

1. Introduction

Superconducting radio-frequency (SRF) cavities are crucial components of modern high-performance particle accelerators to impart energy to the charged particles. Their dramatically lower electrical losses allow operation at substantially higher duty cycles than conventional copper cavities. Accelerators are used for high-energy physics, low-energy to medium-energy nuclear physics research and free-electron lasers. They are also essential tools in industry for industrial processes, in medicine for cancer therapy, for national security, and many additional future accelerator applications are envisioned and under study.

From a mechanical engineering standpoint, a jacketed SRF cavity is typically comprised of an inner niobium vessel (or SRF cavity) surrounded by a liquid helium containment vessel made of stainless steel or titanium. The helium bath may reach pressures exceeding 15 psi (0.103 MPa) and generally has a volume greater than five cubic feet (0.142 m^3). All this leads to consider a jacketed SRF cavity as a system of pressure vessels.

Based on the Department of Energy (DOE) directive 10 CFR 851, it is mandatory for safety reasons that all pressure systems designed, fabricated and tested by U.S. National Laboratories conform to ASME Codes. As a consequence, jacketed SRF cavities fall within the scope of the following sections of the ASME Boiler and Pressure Vessel Code:

- Section VIII - Pressure Vessels, Division 1 and 2
- Section II - Materials, Parts A through D
- Section V - Nondestructive Examination
- Section IX - Welding and Brazing Qualifications

It is acknowledged that a true Code design is not currently possible, primarily due to the use of non-Code materials, the unfeasibility of Code-required nondestructive examinations of welded joints and the use of unqualified procedures for welding and brazing. A set of rules have been developed by engineers at Fermi National Accelerator Laboratory [1] based on their current understanding of best practice in the design, fabrication, examination, testing, and operation of the jacketed SRF cavities. These guidelines comply with Code requirements wherever possible, and for non-Code features, procedures were established to produce a level of safety consistent with that of the Code design.

2. Design Methods for Jacketed SRF Cavities

The mechanical design of jacketed SRF cavities can be approached starting with the ASME BPVC, Section VIII [2, 3]. This section provides detailed requirements for the design, fabrication, testing, inspection, and certification of both fired and unfired pressure vessels. Section VIII contains three divisions, each of which covers different vessel specifications. Division 3 provides rules to pressure vessels that operate at pressures exceeding 10,000 psi. It is not applicable to the design of SRF cavities since they are designed for much smaller working pressures.

Division 1 (Div. 1) is directed at the design of basic pressure vessels, intending to provide functionality and safety with a minimum of analysis and inspection. Common component geometries can be designed for pressure entirely by these rules but they may be not enough for the design of all cavity components under all loading cases (cooldown, additional forces, etc.). Nondestructive examinations (NDE) of welds can typically be avoided by taking a penalty in overall thickness of a component.

Division 2 (Div. 2) is directed at engineered pressure vessels, which can be thought of as vessels whose performance specifications justify the more extensive analysis and stricter material and fabrication controls and NDE required by this Division. The design is governed by two loosely-coupled provisions: Part 4 (Design by Rule), and Part 5 (Design by Analysis). A device may be designed by either Part; regardless of the Part used, the provisions of Parts 3, 6, and 7 (materials, fabrication, and inspection) must be met. The rules of Part 4 are very thorough, duplicating many of the rules of Div. 1, while expanding them to cover a wider range of geometries. The rules of Part 5 provide for a strictly analytical approach to the vessel design. A numerical analysis technique is assumed, and either an elastic or an elastic-plastic analysis is permitted. The mandatory NDE for welded joints in this Division is extensive.

The ASME BPVC Section II is a "Service Section" for reference by the BPVC construction Sections providing tables of material properties including allowable, design, tensile and yield strength values, physical properties and external pressure charts and tables. Part D contains appendices which include criteria for establishing allowable stresses. Some of the materials for the construction of SRF cavities are not accepted by the Code. As a result, the mechanical properties of these materials are not available in Section II, Part D of the Code. Therefore, experimental tests have to be used in the

determination of the material properties for non-Code recognized materials. Subsequently, the material properties determined have to be utilized to calculate the maximum allowable stress values using the Code methodology.

The ASME BPVC Section V contains requirements and methods for non-destructive examination which are referenced and required by other BPVC Sections (i.e. Section VIII). Examination methods are intended to detect surface and internal discontinuities in materials, welds, and fabricated parts and components. Examination per the ASME BPVC is not practical because SRF cavities are constructed of non-Code materials. The ASME Process Piping Code, B31.3, does allow for construction with non-Code materials and is deemed more applicable to the SRF cavity.

The ASME BPVC Section IX contains rules related to the qualification of welding, brazing, and fusing procedures as required by BPVC Section VIII for component manufacture. It also covers rules relating to the qualification of welders, brazers, and welding, brazing and fusing machine operators. The manufacturing of jacketed SRF cavities implies the use of electron-beam welding, gas tungsten arc welding (also known as tungsten inert gas welding), and brazing. Procedures that will guarantee a reasonable level of certainty that the SRF accelerating structure to be fabricated will be in compliance with ASME BPVC must be developed. In each case, if the welded joint or brazed joint is not a standard ASME Code joint, the development must also include sufficient analysis and testing to support the conclusion of equivalent safety. A base set of acceptable weld and braze parameters has to be established for each non-standard joint to assure their integrity examining with a microscope, metallograph or SEM weld and braze samples made by using the contractor's welding/brazing machine. Weld and braze samples for each joint must be as representative as possible: mass, geometry and material thickness, of the actual joint on the structure. Moreover, a sufficient number of samples per weld and braze should be produced to allow tensile tests and bend tests (face and root) at 300 K, 77 K and 4 K. Samples must also be radiographed or ultrasonically examined.

3. SSR1 Case

SRF cavities called Single Spoke Resonators of type 1 (SSR1) are fundamental to the design of a superconducting linear particle accelerator for PIP-II project at Fermi National Accelerator Laboratory [4, 5]. They were

optimized for interactions with proton beam at $\beta = 0.22$ and will operate at 325 MHz in continuous wave (CW) regime.

The jacketed SSR1 cavity consists of two nested cryogenic pressure vessels: the inner vessel is the superconducting SSR1 cavity, see Fig. 1, and the outermost vessel is the helium containment (or helium) vessel, see Fig. 2. The parts of the cavity are formed and machined of high-purity niobium (Nb), and joined by electron-beam welding. Four flanges on the cavity, through which it interfaces with the helium vessel, are made of stainless steel connected to the niobium by means of copper-braze joints. The helium vessel is entirely made of 316L stainless steel and it is assembled around the cavity by full penetration tungsten inert gas (TIG) welds.

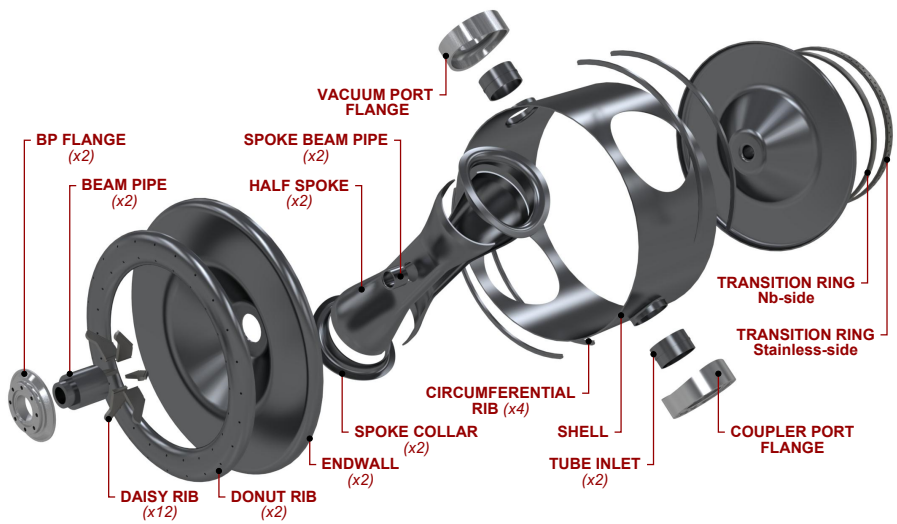

Figure 1: Exploded view of the niobium SSR1 cavity.

The typical operating temperature of an SRF cavity is in the range from 1.8 K to 2.1 K. A bath of superfluid helium, confined by the helium vessel, surrounds the cavity exerting a pressure on both vessels. The RF volume of the cavity is pumped down to ultra-high vacuum, and the entire jacketed cavity is placed in a cryostat under insulating vacuum, see Fig. 5.

The greatest risk with vessels containing superfluid helium is that an accidental loss of vacuum results in very rapid boiling of the helium, causing a consequent pressurization of the helium space. Moreover, differential pressure can be detected between the volumes defined by cavity and helium vessel during the first phases of operation before the cooldown, see Fig. 5. A relief

valve setting of 0.2 MPa is needed to ensure the cavity is protected during initial testing and during cooldown which occur when the cavity is at or near room temperature. A higher rating at low temperature allows the system piping to be sized for higher short-term pressure increases which can occur during a loss of cavity or insulating vacuum when the cavity is cold.

Therefore, the jacketed SSR1 cavity must have two values of maximum allowable working pressure (MAWP), 0.2 MPa at 293 K when the niobium material strength is low, and 0.4 MPa at 2 K when the niobium strength is significantly higher.

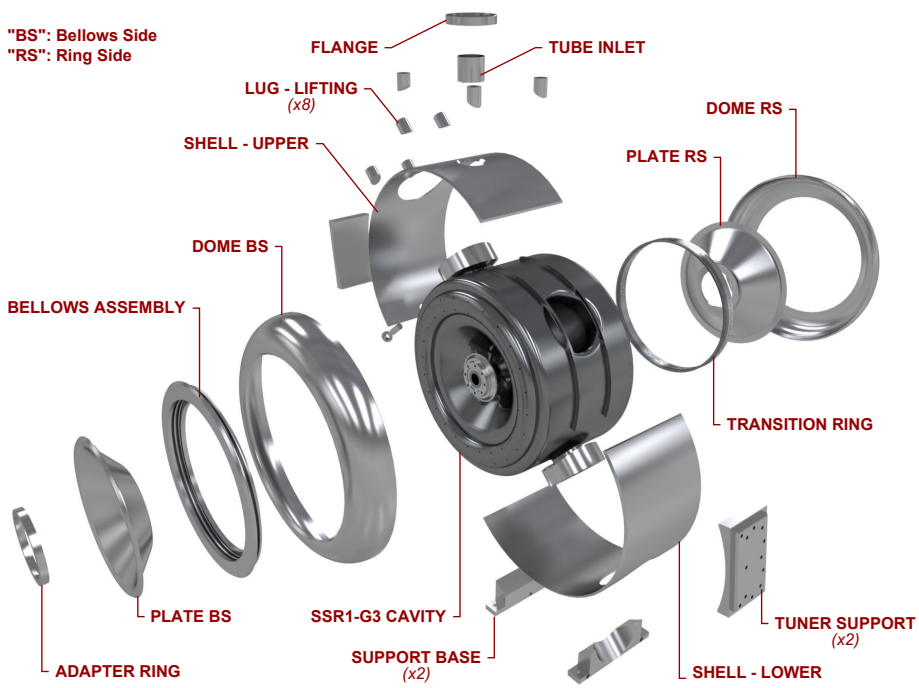

Figure 2: Exploded view of the stainless helium vessel surrounding the SSR1 cavity.

4. Design and Analysis of Jacketed SSR1 Cavity

The need to optimize the complex shape of the jacketed SSR1 cavity under several loading conditions led us to approach the design using Div. 2 of the ASME BPVC Section VIII. The design procedure principally consists of two methods: design-by-rules requirements, described in Part 4, and design-by-analysis requirements, described in Part 5.

The rules of Part 4 were used to provide useful checks of numerical simulations carried out in accordance with Part 5. Part 4.3 was used to set the minimum thickness for elementary geometries such as the cylindrical shell and conical plates of the helium vessel, which are subject to internal pressure[1]. The resulting minimum thickness of the stainless vessel was 2 mm. Part 4.4 was used to set minimum thickness of the cylindrical shell of the niobium cavity, resulting in a wall thickness of 1.5 mm. These minimum thicknesses were used as a starting point for the material optimization, and later increased to ensure stiffness and strength under all loading conditions. Part 4.5 was followed to design nozzles in the shell and heads of the helium vessel subject to internal pressure. Part 4.2 addresses the design of welded joints and was used extensively in the design of the SSR1 system (see section 5). The rules in paragraph 4.19 were applied to the design of a U-shaped unreinforced bellows expansion joint having hydroformed convolutions and two collars welded at the end tangents. The bellows is considered being part of the helium vessel and is made entirely of 316L stainless steel.

The geometries of the structures and loading conditions of SRF cavities, and therefore the stress distributions, are often complicated and do not lend themselves entirely to design by design-by-rules method. The design-by-analysis method can be used to optimize those features not amenable to design-by-rules method. Design-by-analysis method assumes a numerical analysis technique will be used, and either elastic or elastic-plastic analysis is permitted. In the case of the SSR1, ANSYS structural analysis software [6] was used to perform the finite element analyses and provide protection against four modes of failure: plastic collapse, buckling, cyclic loading and local fracture.

4.1. Material Properties

The main structural components of the system are constructed from type 316L stainless steel and ultra-pure niobium. For the analysis, thermal and mechanical properties as well as allowable stresses for both materials are required, at both room temperature and 2 K. While the ASME Code provides Young's modulus (E) and allowable stresses (S) for type 316L stainless at room temperature, it contains no cryogenic properties for this stainless steel, and makes no mention at all of niobium.

[1] In this context, internal pressure is defined as pressure acting on the concave side of the shell

4.1.1. 316L Stainless Steel

Type 316L stainless steel is an ASME Code material. Linear mechanical properties: Poisson's ratio (ν), Young's modulus (E), yield strength (Sy), engineering ultimate tensile stress (Su), as well as allowable stresses (S) for elastic analysis at room temperature are defined in Section II, Part D [7]. However, mechanical properties at cryogenic temperature are not given by the Code. Since the yield strength (Sy) and ultimate stress (Su) of austenitic stainless steels increases substantially at cryogenic temperatures, a conservative approach was chosen and room temperature properties were used, see Table 1. Additionally, the coefficient of thermal expansion (CTE) over the wide temperature range from 293 K to 2 K is not available from the Code, but is well known in literature [8, 9].

The elastic-plastic stress strain curve required for the plastic collapse analyses, shown in Fig. 3, was derived from the Ramberg-Osgood correlations, which use the Code yield and ultimate stresses in combination with other parameters provided by Div. 2, Part 3, Annex 3.D [3].

Table 1: Mechanical properties of type 316L stainless steel.

T[K]	E[GPa]	ν	Sy[MPa]	Su[MPa]	S[MPa]
293	195	0.30	172	517	114
2	Conservatively assumed equal to 293 K properties				

4.1.2. Niobium

The ultra-pure niobium (300 RRR) is a non-Code material. Several sheet-type specimens of bulk niobium, heat treated, and electron beam welded were tensile tested at room temperature (293 K) at St. Louis Testing Laboratories following the standards ASTM E8-04. The specimens were wire EDM cut from a 3.1 mm thick sheet. Gripping devices for sheet specimens were used to transmit the measured force applied by the testing machine to the test specimens, and to ensure that the axis of the specimen coincided with the center line of the heads of the testing machine. An axial clip-on extensometer was employed to measure the elongation of the specimens. The offset method was used to determine yield strength (Sy). The ultimate stress (Su) was calculated by dividing the maximum force carried by the specimen during the tension test by the original cross-sectional area of the specimen.

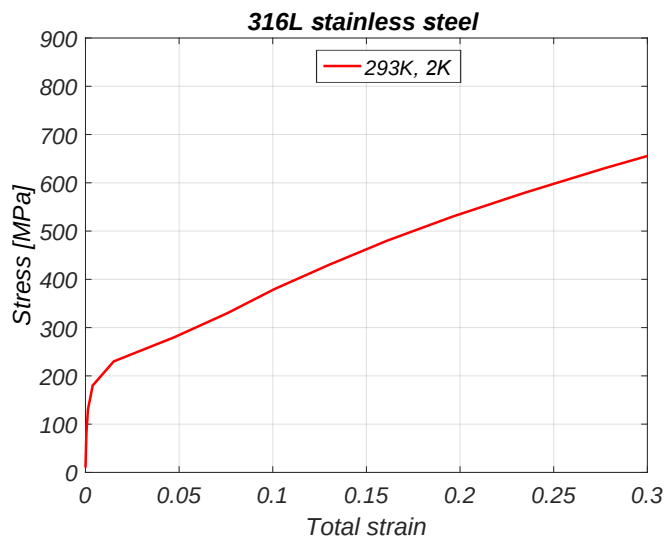

Figure 3: Stress strain curve for 316L stainless steel derived from the Ramberg-Osgood correlation using the following fitting parameters $m_2 = 0.75(1.00 - R)$ and $\epsilon_p = 2 \times 10^{-5}$.

The lowest (conservative) values of yield strength (Sy) and ultimate stress (Su) were used to define the allowable stress[2] (S). The highest value of Young's modulus (E) was employed because it produces higher stresses in strength analyses, which take into account the most critical failure modes of such type of structures. Literature data [1, 10] were used to define the mechanical properties of pure niobium at cryogenic temperature, including the coefficient of thermal expansion (CTE) from 293 K to 2 K [9]. See Table 2.

The elastic-plastic stress strain curves at both 293 K and 2 K, shown in Fig. 4, were derived from the Ramberg-Osgood correlations (see Annex 3.D of the Code [3]). However, since niobium is not a Code material, parameters specific to it were not available. Instead, the parameters for titanium were used. The possibility of using copper parameters was explored, but it was found that even though the difference between the two curves was very small, the behavior near the yield point was slightly less conservative with copper parameters.

[2]The allowable stress (S) was defined according to Table 1-100 of the Code [7].

Table 2: Mechanical properties of pure niobium.

T[K]	E[GPa]	ν	Sy[MPa]	Su[MPa]	S[MPa]
293	105	0.38	74	160	46
2	105	0.38	317	600	171

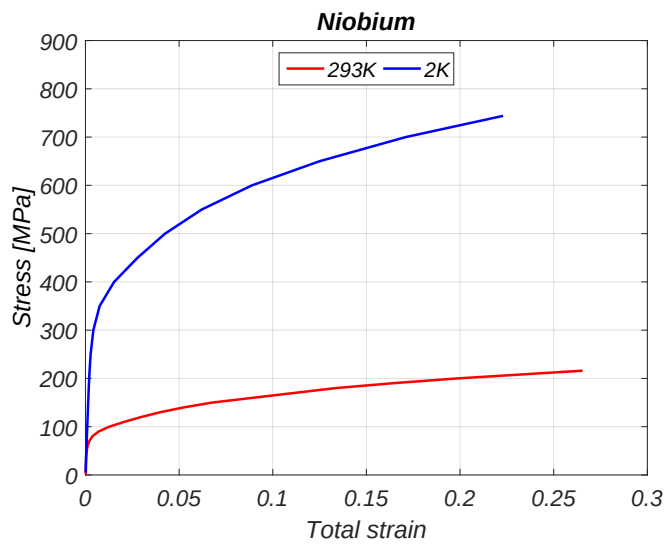

Figure 4: Stress strain curves for pure niobium derived from the Ramberg-Osgood correlation using the following fitting parameters $m_2 = 0.50(0.98 - R)$ and $\epsilon_p = 2 \times 10^{-5}$.

4.1.3. Material of Brazed Joints

The connections between niobium and stainless steel were made adopting a copper-brazed transition technique [11]. The filler metal is oxygen free electronic copper (CDA-101). Full scale samples were constructed and qualified through a series of leak tests, load tests, thermal cycling, visual and microscopy (SEM) inspection [12]. Results from tensile tests on brazed specimens were taken into account to define the allowable stress (S), see Table 3. The allowable stress was defined according to Table 1-100 of the Code [7]. Load tests at cryogenic temperature were not performed but it is reasonable to assume that the static mechanical properties are higher than at room temperature. Thus, to be conservative, the allowable stress at cryogenic temperature was assumed equal to the value at room temperature.

Table 3: Mechanical properties of copper-brazed joints.

T[K]	E[GPa]	ν	Sy[MPa]	Su[MPa]	S[MPa]
293	–	–	–	120	34
2	Conservatively assumed equal to 293 K properties				

4.2. Loads and Load Case Combinations

According to Table 5.5 of Div. 2, the loads applied to SSR1 system have been identified (see Fig. 5) and they are:

P - Pressure into the helium space to satisfy the conditions of MAWP = 0.2 MPa at 293 K and MAWP = 0.4 MPa at 2 K

p_{He} - Static head from liquid helium (considered as negligible)

p_{rf} - radiation pressure acting on the niobium walls produced by RF power in CW regime at the maximum accelerating gradient of 12 MV/m (considered as negligible)

D - Dead weight of the vessel and cavity: 1250 N

T_1 - Elastic tuning, maximum displacement of 0.26 mm of the beam pipe

T_2 - Cooldown from 293 K to 2 K

Four load cases have been defined and reported in Table 4 to study all critical conditions that might occur to the SSR1 system. Load cases 1 and 2 are representative of the critical scenarios at room temperature (293 K), where the system is stressed by dead weight (D), a maximum of 0.2 MPa of differential pressure (P) into the helium space, and maximum displacement of the beam pipe (T_1) to allow resonant frequency adjustment by a mechanical "tuner" [13]. The worst scenarios of loading at 2 K are described by load cases 3 and 4, where the system is subject to thermal stresses due to the cooldown (T_2), the dead weight (D), a maximum of 0.4 MPa of differential pressure (P) into the helium space, and maximum action of the tuner (T_1).

In the cryomodule the jacketed cavity is principally constrained by the support bases bolted to the plate of the support post that is made of the same material (no differential thermal contraction). In the FE model, a

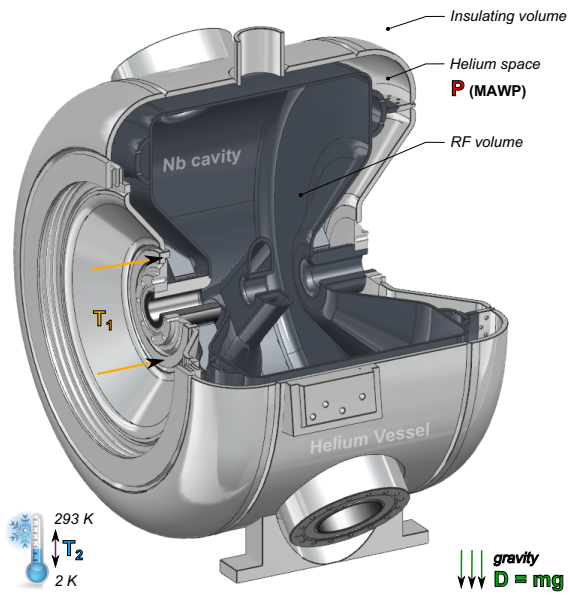

Figure 5: Jacketed SSR1 system with schematic loads applied. The pressure (P) is applied normal to the surfaces defining the helium space, the frequency tuning displacement (T_1) is applied normal to the beam pipe (along the arrows), the gravitational force (D), and the cooldown (T_2) applied to the entire system.

set of "0-displacement" in the three principal directions, instead of "fixed support", was applied on the support bases (see Fig. 2) to avoid localized stresses during the cooldown.

Table 4: Load cases and design temperature used to study the behavior of the SSR1 system. Load combination factor will be applied for specific analyses.

Case 1	Case 2	Case 3	Case 4
$P + D$	$P + D + T_1$	$P + D + T_2$	$P + D + T_1 + T_2$
293 K	293 K	2 K	2 K

4.3. Protection Against Plastic Collapse

The analysis for this failure mode focuses on the internal pressure of the vessel and prevents plastic instability, ensuring that the pressure vessel does not experience plastic deformation that may lead to collapse. Moreover,

Table 5: MAWP for plastic collapse analyses.

Case 1	Case 2	Case 3	Case 4
$P + D$	$P + D + T_1$	$P + D + T_2$	$P + D + T_1 + T_2$
0.244 MPa	0.323 MPa	0.897 MPa	0.897 MPa

the analysis avoids unbound displacement in each cross-section of the SSR1 system.

Three separate approaches are permitted by Div. 2, Part 5.2, for protection against plastic collapse: elastic stress analysis, limit load analysis, and elastic-plastic analysis. The elastic-plastic stress analysis method was chosen, as it permits the most sophisticated material property characterization, and is likely to produce the highest MAWP.

4.3.1. Elastic-Plastic Stress Analysis Method

The Load Combination Factor (LCF) for each load case is defined using Table 5.5 of Div. 2, having $LCF = 2.4$ for load cases 1 and 2, and $LCF = 2.1$ for load cases 3 and 4.

Elastic plastic analyses were performed for each load case combination by applying the loads in two steps. In the first step, the factored dead weight, thermal contraction, and tuner displacement were applied. In the second load step only the pressure was applied, and increased incrementally until collapse (i.e., failure of the finite element model to converge) occurred. The MAWP was then calculated by dividing the value of pressure at the last converged solution by the LCF. Table 5 summarizes the values of MAWP for the SSR1 system determined for each load case combination using this approach. Fig. 6 shows the location where the failure initiates in all load cases. In all listed cases, the values of MAWP are always above the specified requirements.

4.4. Protection Against Local Failure

Protection against local failure is directed at identified regions of high triaxial stress, which may not produce significant von Mises stress, but could produce tensile strains sufficient to fracture the material. By Part 5, paragraph 5.3 protection against local failure may be assessed by either elastic analysis, or elastic-plastic analysis.

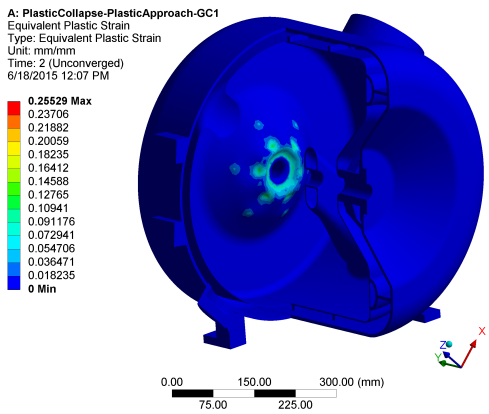

Figure 6: The failure due to plastic collapse initiates on the highlighted area of the niobium cavity.

The elastic analysis approach was chosen for this work. Paragraph 5.3.2 states that, for each point in the component, the following condition must be met:

$$(P_1 + P_2 + P_3) \leq 4S \tag{1}$$

where P_1, P_2, and P_3 are the principal stresses, and S is the allowable stress. Very little guidance is given for implementation, other than that the primary local membrane plus bending stress is to be used for the evaluation. This implies that peak stresses need not be considered.

For this analysis, it was decided that it would be conservative to consider each finite element as a "point", since this would include peak stress effects. A macro was written in ANSYS to extract the centroidal values of the principal stresses in each element of the model, and used to verify that the requirement expressed above by Eq. 1 was satisfied. All shells, formed heads and ribs on the cavity and the helium vessel passed the criterion as enforced here, for all load case combinations.

4.5. Protection Against Collapse from Buckling

Structural instability, or buckling, can lead to the sudden failure of a mechanical component. The load at which buckling occurs depends on the stiffness of the component, not on the strength of its materials, and the loss of stability can happen even when component stresses are in the linear elastic range.

Table 6: Results from linear buckling analyses.

Case 1	Case 2	Case 3	Case 4
$P + D$	$P + D + T_1$	$P + D + T_2$	$P + D + T_1 + T_2$
$\Phi_B = 16.75$	$\Phi_B = 16.5$	$\Phi_B = 7$	$\Phi_B = 7$

For the SSR1 system, the thin-walled niobium cavity (2.8 mm) is under compressive stress from external pressure, and is therefore susceptible to buckling.

The effects of initial imperfections of geometry were not considered in the plastic collapse analysis. When such imperfection are included, Part 5, paragraph 5.4 does not require a separate buckling analysis, since the maximum effects of out-of-roundness, etc., would have been included in the plastic collapse calculation. However, it is permitted to perform a separate linear buckling (bifurcation, or Euler buckling) analysis on the "perfect" geometry, provided the required design factors are adhered to.

4.5.1. Bifurcation Buckling Analysis - Type 1

The design factor is based on the type of buckling analysis performed and in this case it shall be:

$$\Phi_B \geq \frac{2}{\beta_{cr}} = 2.5 \tag{2}$$

A capacity reduction factor $\beta_{cr} = 0.8$ was chosen because the most probable area of collapse in the SSR1 system (the shell) is similar to an unstiffened cylinder.

The four load cases shown in Table 4 were applied in the pre-stress load conditions. For each one of them the load design factor was calculated and is reported in Table 6. In all of the listed cases, the safety factor on buckling always satisfies the design factor of Eq. 2, and the first component to buckle is the shell of the niobium cavity, as shown in Fig. 7.

4.6. Protection Against Failure from Cyclic Loading

Paragraph 5.5 of Part 5 provides procedures to ensure protection against failure under cyclic loading. Two types of cyclic loading are addressed: fatigue, and ratcheting. In the case of fatigue, a screening procedure is presented to determine if the number and magnitude of stress cycles is enough to require a full fatigue analysis.

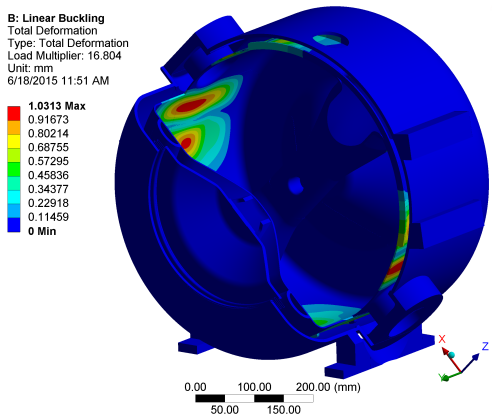

Figure 7: Failure due to buckling initiates on the red marked area of the niobium cavity.

4.6.1. Fatigue Analysis Screening, Method A

In SRF structures, fatigue cycles result from frequency adjustments (tuning cycles, T_1) and temperature changes (cooldown/warmup, T_2). Frequency tuning comprises "coarse tuning" and "fine tuning". The contribution of fine tuning is not considered in the analyses because of its small amplitude.

Paragraph 5.5.2 provides two screening methods to determine if a fatigue analysis is required. Method A can be used for materials with a specified minimum tensile strength that is less than or equal to 552 MPa. This is not the case for niobium at cryogenic temperature, where $S_u = 600\,\text{MPa}$. However, Method B, which does not have restrictions on material strength, requires the use of a fatigue curve generated by the procedures of Annex 3.F of Part 3, Div. 2. The parameters for generating this curve are material-specific, and because niobium is not a Code material, no parameters are available. It was decided, since both methods require stepping outside the strict boundaries of the Code, that Method A would be the best choice for determining if a fatigue analysis is required for jacketed SSR1 cavities.

Step 1. Determine the load history.
There are three loads in the load history: pressure (P), tuning cycles (T_1) and cool down/warm-up (T_2).

Step 2. Determine the expected number of full-range pressure cycles including startup and shutdown, $N_{\Delta FP}$.
The SSR1 system will undergo a maximum of 3 cooldown/warmup cycles during commissioning and an additional 1 cycle for each year of

operation. Assuming an operating life of 40 years, the total number of warmup-cooldown cycles will be $N_{\Delta FP} = 43$.

Step 3. Determine the expected number of operating pressure cycles in which the range of pressure variation exceeds 20% of the design pressure for integral construction $N_{\Delta PO}$.
There will be no operation of an SSR1 system at a pressure deviating 20% from the design pressure. Therefore, $N_{\Delta PO} = 0$.

Step 4. Determine the effective number of changes in metal temperature difference between any two adjacent points, ΔT_E.
The effective number of such changes is determined by multiplying the number of cooldown by two: $N_{\Delta TE} = 43 \cdot 2 = 86$.

Step 5. Determine the number of temperature cycles for components involving welds between materials having different coefficients of thermal expansion ($N_{\Delta T\alpha}$) that causes the value of $(\alpha_1 + \alpha_2)\Delta T$ to exceed 0.00034.
For the SSR1 system, $N_{\Delta T\alpha} = 43$.

Step 6. Determine the number of course tuner cycles expected during the system's lifetime, $N_{\Delta T_1}$.
There are assumed to be 10 coarse tuner cycles per year for 40 years of operations. Therefore, $N_{\Delta T_1} = 400$.

Step 7. If the expected number of operating cycles from steps 2-6 satisfies the criterion of Table 5.9 of the Div. 2, then no fatigue analysis is required.
The criterion of Table 5.9 requires the sum of the operating cycles steps 2-5 to be equal to or less than 1000. The sum for the SSR1 system is 572 cycles. Therefore, per Method A, no fatigue analysis is required.

4.6.2. Ratcheting Assessment - Elastic-Perfectly Plastic Analysis

Two analysis methods are allowed by Div. 2 for the ratcheting assessment: Elastic Stress Analysis (Part 5.5.6) and Elastic-Plastic Stress Analysis (Part 5.5.7). For the SSR1 case, an elastic-plastic stress analysis was performed since a model for the analysis that accurately represents the component geometry, boundary conditions, applied loads, and material properties was already developed for previous analyses.

The analysis for protection against ratcheting is performed by application, removal and re-application of the applied loadings to show that the structure eventually shakes down to elastic action, i.e., that the incremental increases

in plastic deformations from each cycle are small and diminishing as the number of cycles increases.

The finite element model was subjected to 20 load cycles. Each load cycle consisted of the following eight-steps:

1. Warm pressurization, $P = 0\,\mathrm{MPa} \rightarrow 0.2\,\mathrm{MPa}$
2. Thermal cooldown, $T_2 = 293\,\mathrm{K} \rightarrow 2\,\mathrm{K}$
3. Extension of tuner, $T_1 = 0\,\mathrm{mm} \rightarrow 0.25\,\mathrm{mm}$
4. Cold pressurization, $P = 0.2\,\mathrm{MPa} \rightarrow 0.4\,\mathrm{MPa}$
5. Cold depressurization, $P = 0.4\,\mathrm{MPa} \rightarrow 0.2\,\mathrm{MPa}$
6. De-extend tuner, $T_1 = 0.26\,\mathrm{mm} \rightarrow 0\,\mathrm{mm}$
7. Warm-up to room temperature, $T_2 = 2\,\mathrm{K} \rightarrow 293\,\mathrm{K}$
8. Warm depressurization, $P = 0.2\,\mathrm{MPa} \rightarrow 0\,\mathrm{MPa}$

Using ANSYS, several deformation probes were established on the geometry in the most stressed and/or deformed areas. The deformations at the probe locations were used to examine whether distortions were increasing or decreasing during the cycle. Three of them are shown in Fig. 8.

It should be noted that there are two very conservative assumptions in this analysis. The first is the elastic-perfectly plastic material model, which essentially limits the maximum stress of any element to the yield strength of the material. In reality, both the stainless steel and niobium demonstrate considerable post-yield stiffness. The second conservative assumption is the use of failure-mode maximum pressures at every cycle, as well as maximum tuner displacements. It is unlikely that the cavity will be subjected to twenty cycles of this severity during service[3].

Satisfying any one of the following three criteria is sufficient to demonstrate protection against ratcheting:

1. There is no plastic action in the component.
2. There is an elastic core in the primary-load-bearing boundary of the component.
3. There is not a permanent change in the overall dimensions of the component.

[3]The cavities will reach or exceed the MAWP (overpressurized condition) in case of accident: loss of cooling with subsequent loss of helium to atmosphere. Experienced scientists at Fermilab say "we expect one incident within 2 to 10 year period". In our analyses we have conservatively considered the worst case scenario: 1 incident/year.

As seen in Fig. 8, convergence to pure elastic action cannot be obtained in twenty cycles. However, all trends are smooth, and eventual convergence can be safely assumed. This behavior confirms the existence of an elastic core, meeting the requirements of the Code. The final permanent deformations of the probe locations at the end of 20 load cycles must be regarded as absolute upper limits. It is highly unlikely that these limits will be reached in practice, due to the very conservative assumptions made in this analysis.

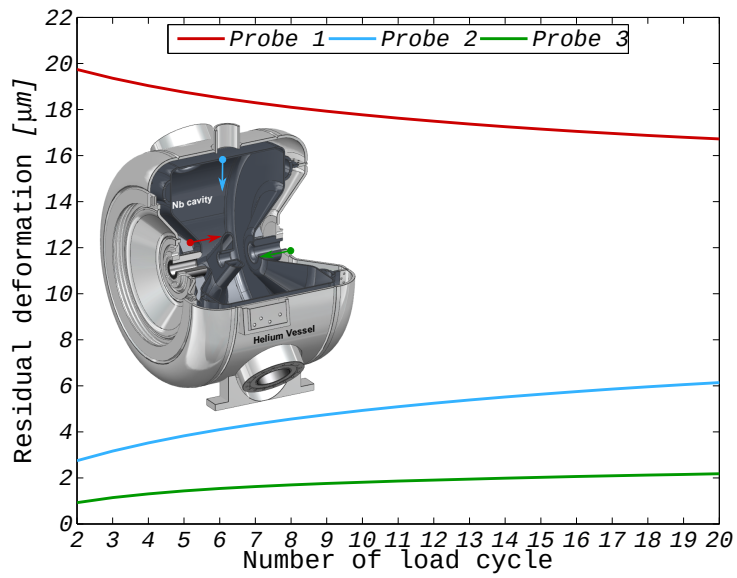

Figure 8: Residual plastic deformation between load cycles in the direction of the probes. The displacements are taken from load step 8 of each cycle, in which the system is entirely unloaded, and represent permanent deformations.

5. Design of Permanent Joints

The types of welds joining stainless steel parts are defined in paragraph 4.2 of Div. 2. However, since nondestructive inspections are not performed, joint efficiencies for unradiographed welds, given in Div. 1 - Table UW-12, have been adopted. All TIG welds are classifiable as single-welded butt joints with backing strip, and single full fillet lap joints, which have weld efficiencies (ϵ) of $\epsilon = 0.65$ or $\epsilon = 0.45$, respectively.

It was not possible to strictly adhere to Code rules in defining the types of welds used for joining the niobium parts because of the stringent requirements for the high-quality surfaces in SRF components. Several welded samples were made to define and achieve the best welding parameters. The samples were etched and studied microscopically, their integrity (absence of defects) was verified and the effective weld areas, A_{eff}, measured. This level of inspections has led to the conclusion that the weld efficiency $\epsilon = 1$ is appropriate for niobium electron-beam joints.

The same approach was used to qualify the copper brazed joint, for which ϵ is also taken as 1.

The integrity of the cavity structural connections was verified using the results of finite element analyses performed with models having bonded contact between parts, i.e., welding beads or brazed interfaces were not explicitly modeled. A linear elastic analysis was performed for all four load case combinations (see Table 4) and the stress state at connections assessed by hand calculations. The level of criticality of each permanent joint was defined by the design safety factor $\eta = \sigma_{eq}/S$. The von Mises stress, σ_{eq}, was calculated from the nodal forces acting on the joints, extracted from the finite element analyses, divided by the effective weld area, A_{eff}. The joint was considered safe if the condition $\eta\epsilon > 1$ was met.

All joints passed the safety requirement $\eta\epsilon > 1$. In addition, stress classification lines (SCLs) were created through the more highly stressed joints to support the hand calculations. Fig. 9 shows the SCL through the most highly stressed niobium electron-beam joint and confirms the verification approach, with an error between the hand calculated stress and the simulation result that is less than 10%. The stress distribution, linearized by ANSYS in the manner specified by Part 5 of Div. 2 of the Code, satisfies the safety conditions $\sigma_M/\varepsilon \leq S\epsilon$ and $\sigma_{M+B}/\varepsilon \leq 1.5S\epsilon$.

The inclusion of weld efficiencies (characteristic of Div. 1 vessel design, where radiography is not mandatory) should permit this analysis to stand as qualification of the vessel under the provisions of U-2(g) of Div. 1.

6. Inspection and Examination

All examination requirements of the Code (e.g., weld examination) have not been strictly followed in the construction of the jacketed SSR1 cavity. However, a combination of visual examinations, radio-frequency measurements, and leak checks confirms the integrity and reliability of the niobium

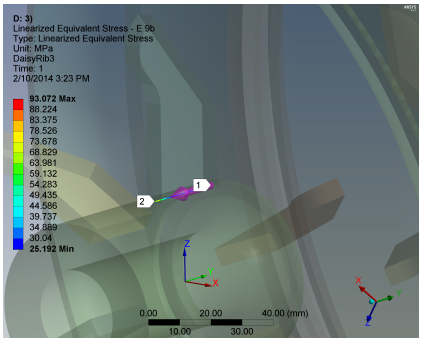

(a) Stress classification line (SCL)

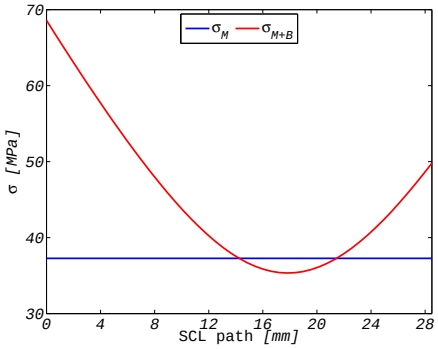

(b) Linearized stresses on the SCL: membrane stress σ_M and membrane plus bending stress σ_{M+B}

Figure 9: SCL through the more stressed electron beam welded joint.

cavity and stainless steel vessel.

Visual examination at each critical step was performed in order to prevent visible defects in the parts. All welds for pressure retaining parts were visually examinated by manufacturer personnel under the supervision of Fermilab inspectors to assure the acceptance criteria of Table 7.6 of the ASME BPVC, Section VIII, Div. 2, Part 7. The electron-beam welds joining niobium parts are also examined from inside of the cavity (radio-frequency volume) with the aid of a video scope. TIG welds for stainless parts are visually examined step-by-step during the highly-controlled process of welding. Integrity of braze joints is visually checked looking at both ends of the joint with a glass magnifier to exclude the presence of defects. None of the joints were subject to NDE. Proper efficiency coefficients for joints design were taken into account to overcome the absence of NDE. Joints having a design that does not meet the rules of the ASME BPVC were qualified by testing samples of the same specific joint to prove the manufacturing process and material.

Measurements of the resonant radio-frequency are extremely important in obtaining a jacketed SRF cavity with the proper frequency at each step. They are also used to monitor the deformations of the niobium cavity during machining and welding, preventing plastic deformations which are above acceptable limits. This is possible because the resonant radio-frequency of a given volume shifts as the volume varies, with sensitivity on a nanometer scale.

Several leak checks of the vessels were performed at various stages of the fabrication in order to prove that all welds and brazed joints are leak tight with a minimum sensitivity of 10^{-9} atm·cc/s. Parts and final assemblies were measured using a coordinate measuring machine to check the geometrical properties of the objects and their adherence to released drawings. Material certifications are provided by the manufacturers to prove the specified quality and grade of the material.

7. Pressure Testing

Pressure testing shall be performed per the ASME BPVC, Section VIII, Div. 2, Part 8 when the vessels are completely welded, machined and inspected. The validity of the design approach used for the jacketed SSR1 cavity, in terms of safety, reliability and leak tightness has been ensured through a pneumatic pressure test. All safety precautions were adopted before and during the execution of the test.

The helium space was pressurized at the test pressure of 1.15 times the MAWP at room temperature, $P_T = 0.23\,\mathrm{MPa}$, according to Part 8.3 of the Code. The absence of leaks was proved by monitoring the pressure, which must be constant for the 10 minutes duration of the test. An additional check was done to detect plastic deformations of the niobium cavity (the weakest vessel) by measuring the shift of the resonant radio-frequency during the test. Comparing the value of the frequency after two pressurization cycles showed no shift in frequency, confirming the absence of plastic deformation due to the pressure test.

A helium leak check with a minimum system background of $10^{-9}\,\frac{atm \cdot cc}{s}$ was performed after the pressure test and verified the absence of leaks at welds, seals, in other possible locations.

8. Conclusion

The SSR1 design case is an example of a jacketed SRF cavity designed using the rules of ASME BPVC, Section VIII, Div. 2. Some of the most common non-compliances have been addressed using "equivalent rules" in terms of safety, when the Code does not apply.

The use of different technologies and materials in the design and fabrication of the various styles of SRF cavities does not allow the definition of a single, unique procedure that could be extended to all SRF cavities.

Nevertheless, the design of other jacketed SRF cavities may be approached using the set of rules reported in this paper, as a starting point to meet Code requirements at the greatest extent possible.

Acknowledgment

The activities described in this paper are supported by Fermi Research Alliance, LLC under Contract No. DE-AC02-07CH11359 with the United States Department of Energy.

References

[1] Guidelines for the Design, Fabrication, Testing and Installation of SRF Cavities, FESHM Chapter 5031.6, TD-09-005, Fermi National Accelerator Laboratory

[2] ASME Boiler and Pressure Vessel Code, Section VIII - Rules for Construction of Pressure Vessels, Division 1, 2010

[3] ASME Boiler and Pressure Vessel Code, Section VIII - Rules for Construction of Pressure Vessels, Division 2 - Alternative Rules, 2010

[4] L. Ristori et al., "Development and Performance of 325 MHz Single Spoke Resonators for Project X", Proceedings of SRF 2013, Paris, France

[5] T. Nicol et al., "SSR1 Cryomodule Design for PXIE", Proceedings of PAC2013, Pasadena, USA

[6] ANSYS Academic Research Mechanical, Release 16.0, ANSYS, Inc.

[7] ASME Boiler and Pressure Vessel Code, Section II, Part D, Materials, 2010

[8] 316 Stainless Steel Material Properties NIST, Cryogenic Technologies Group

[9] J.E. Jensen, et al., "Selected cryogenic data notebook, Volume II, Sections X-XVIII", BNL

[10] T.J. Peterson et al.,"Pure Niobium as a Pressure Vessel Material", FERMILAB-PUB-09-320-TD, Fermi National Accelerator Laboratory

[11] J.D. Fuerst et al., "Niobium to Stainless Steel braze transition development", Proceeding of SRF 2003, Lubeck, Germany

[12] L. Ristori et al., "Development at ANL of a copper-brazed joint for the coupling of the niobum cavity end wall to the stainless steel helium vessel in the Fermilab SSR1 resonator", Proceedings of IPAC 2012, New Orleans, USA

[13] D. Passarelli et al., "SSR1 Tuner Mechanism: Passive and Active Device", Proceedings of LINAC 2014, Geneva, Switzerland